International Journal of Food Microbiology 300 (2019) 31–42

Contents lists available at ScienceDirect

International Journal of Food Microbiology

journal homepage: www.elsevier.com/locate/ijfoodmicro

Optimization of bioactive preservative coatings of starch nanocrystal and ultrasonic extract of sour lemon peel on chicken fillets

Zahra Alizadeh[1], Shima Yousefi*, Hamed Ahari[1]

Department of Food Science and Technology, Science and Research Branch, Islamic Azad University, P.O. Box 1476714171, Tehran, Iran

ARTICLE INFO

Keywords:
Antimicrobial
Antioxidant
Polymeric solution
Shelf lifesour
Lemon peel
Starch nanocrystal

ABSTRACT

Starch nanocrystal (S-NC) was produced after sulfuric acid hydrolysis of potato starch granules and then characterized by laser diffraction particle size analyzer, scanning electron microscopy (SEM) and X-ray diffraction (XRD). Response surface methodology (RSM) was applied to optimize S-NC (2–10%) concentration, sour lemon peel extract (SLPE, 2.5–12.5%) amount, mixing temperature (M-TE, 25–65 °C) and mixing time (M-TI,15–75 min) in the preparation of bioactive coating solutions to develop the high-quality chicken fillets during the cold-storage. The optimized conditions for achieving the highest DPPH· inhibition percentage (89.14%), antibacterial activity (*Staphylococcus aureus*, 3.58-mm; *Escherichia coli*, 3.14-mm; *Listeria monocytogenes*, 2.31-mm and *Salmonella enterica*, 2.24-mm) and lightness value (77.82) and the lowest redness (6.69), yellowness (13.21) values and viscosity (27.5 mPa.s) were 4.0% S-NC, 5.62% SLPE, 51.17 °C M-TE and 43.29 min M-TI. Spraying the optimal coating solution on chicken fillets led to a significant improvement in their physico-chemical, textural and sensory characteristics compared to the control during 12-day cold-storage.

1. Introduction

In recent years, the demand for the consumption of available and high-quality poultry meats has been increasing rapidly in many countries of the world. This popularity is due to their relatively inexpensive production and high diversity of commercially processed products with a low fat content, a high nutritional value and a distinguished flavor (Khare et al., 2017; Latou et al., 2014). Accordingly, the development of biocompatible methods to improve the storagability of poultry meat-based products is one of the main aims of the poultry industry to assign large part of the target national and international markets. The novel preservative technologies and strategies, such as modified atmosphere packaging and edible and biodegradable films and coatings, aiming at the lowest changes of physicochemical, textural and sensory characteristics of poultry meats during cold storage have been currently utilized (Latou et al., 2014; Umaraw and Verma, 2017). In addition, the incorporation of functional natural extracts with excellent antioxidant and antimicrobial activities into packaging materials is taken into consideration to prolong the shelf life of a wide spectrum of these meat products (Choulitoudi et al., 2016).

One of the most common ready-cooked meat products is chicken fillet which is a skinless and boneless chicken breast. Extending this economical product by natural preservatives not only can maintain its critical quality parameters, but also can potentially decrease hazards of the use of chemical additives (Owens et al., 2010). Since biodegradable polymers extracted from plant and animal tissues are relatively low-cost and eco-friendly, they can be easily used to highly-efficient preserve chicken fillets in term of edible films or coatings (Khare et al., 2017).

Starch is a polymer of glucose molecules with two structural parts of long, highly branched (amylopectin) and short, linear (amylose). The special hydrolysis of amorphous regions of this polymer can isolate the crystalline regions to prepare starch nanocrystals (S-NCs) with the size of ≤100 nm (Lin et al., 2011a, 2011b). These nanoscale platelets with the high crystallinity are able to improve barrier and physico-chemical characteristics of bio-composites to package a high number of food materials (Basiak et al., 2017). Although the capability of S-NCs in developing bio-plastics (González et al., 2015; Mukurumbira et al., 2017) and Pickering emulsions (Ge et al., 2017; Liang et al., 2016) has been recently proved, there is no specific study on the use of nano-materials to form preservative coating solutions.

It has been demonstrated that the combination of starch and its derivatives with antimicrobial agents in the formulation of edible films can significantly lengthen shelf life of meat products (Bof et al., 2016; Hari et al., 2017; Lozano-Navarro et al., 2017). Sour lemon peel (SLP) as a low-cost and much frequently available waste material is mostly used to extract pectin. However, the aquoues extract of this citrus by-

* Corresponding author.
E-mail address: Shyousefi81@gmail.com (S. Yousefi).
[1] Zahra Alizadeh and Dr. Hamed Ahari should be considered as first authors and contributed equally to this research.

https://doi.org/10.1016/j.ijfoodmicro.2019.04.002
Received 24 October 2018; Received in revised form 26 March 2019; Accepted 3 April 2019
Available online 05 April 2019
0168-1605/

product due to the having antimicrobial and antioxidant characteristics (Ruiz et al., 2016) can be considered as a bioactive constitute in the improvement of functionality of S-NC based packaging coatings.

However, there is a serious requirement to determine the exact ratio of S-NC and SLP extract and also their mixing conditions. Response surface methodology (RSM) with a collection of mathematical and experimental techniques is a powerful tool to optimize formulation and processing parameters even in the presence of complex interactions. The determination of optimized response surfaces by RSM is implemented with a limited number of experimental trials, and the low development time and overall cost (Yousefi et al., 2015).

Therefore, the aim of this study was to optimize innovative functional coating solutions based on the mixture of S-NC and SLP extract using RSM in order to extend the shelf life of high-quality chicken fillets stored under the refrigerated conditions.

2. Materials and methods

2.1. Raw materials

Sour lemon fruits were obtained from the Citrus Research Station (Jahrom, Iran). After the washing whole fruits, their peel was separated using a knife and dried in a lattice tray using an oven at 40 ± 1 °C for 48 h. The dried peels were ground using a Moulinex coffee grinder (Moulinex Ltd., Coulsdon, Surrey, England) and the obtained powders were passed through a sieve (mesh #60, cut-off size of ~250 μm). Commercially fresh chicken breast fillets were purchased from a local market in Tehran (Iran) and then stored in a refrigerator at 4 ± 1 °C for further experiments.

2.2. Chemicals and reagents

Ethanol (96%) was supplied by Razi Chemical Co. (Tehran, Iran). Other chemicals such as potato starch, methanol, 1-butanol, sodium hydroxide (NaOH), hydrochloric acid (HCl), malondialdehyde (MDA), sulfuric acid, thiobarbituric acid, phenolphthalein and 2,2-diphenyl-1-picrylhydrazyl (DPPH·) were provided by Merck Chemical Co. (Darmstadt, Germany).

2.3. Microorganisms and culture media

Freeze-dried four microorganisms of *Staphylococcus aureus* PTCC 1189, *Escherichia coli* PTCC 1330, and *Listeria monocytogenes* PTCC 1298 were purchased from the Persian type culture collection of the "Iranian Research Organization for Science and Technology (IROST, Tehran, Iran)". *Salmonella typhimurium* ATCC 14028 donated by "Islamic Azad University, Saveh Branch, Iran" The nutrient agar and Mueller-Hinton agar (MHA) plate were provided by Merck Chemical Co. (Darmstadt, Germany). Stock cultures of the tested bacteria were grown in MHA at 37 °C for 24 h prior to the experiments.

2.4. Starch nanocrystal (S-NC) preparation

The modified method of Angellier et al. (2004) was applied to prepare S-NCs from potato starch granules (PSGs). An aqueous solution of sulfuric acid (250 mL) was used to hydrolyze PSGs at 40 °C and 100 rpm for 5 days. After completing the hydrolysis time, the obtained S-NCs were separated from the acidic aqueous suspension using a centrifugation system (Hettich Zentrifugen, EBA-20 model, Germany) at 10,000 rpm and 4 °C for 15 min. Subsequent wash-centrifugation cycles were carried out to ensure the eluent neutrality. An ultrasonic homogenization treatment (ultrasonic homogenizer, FAPAN, Iran) for 10 min at frequency of 24 kHz was then performed to have a uniform distribution of S-NCs in the colloidal suspensions. The aqueous S-NCs suspension was finally sprayed into a mini spray dryer chamber (Büchi B290, Flawil, Switzerland) in order to produce S-NC powders.

2.5. S-NCs characterization

2.5.1. Particle size and morphology of S-NCs

A commercial Malvern Zetasizer Nano ZS (Malvern Instruments Ltd., Malvern, UK) was utilized to measure the size of S-NCs at 25 °C. The microstructure of S-NCs was evaluated by means of a scanning electron microscope (SEM, XL 30, Philips, Eindhoven, Netherlands). Dried powders of S-NC were mounted on the specimen holder by a double-sided adhesive tape and lastly sputtered with gold using a sputter coater (BAL-TEC AG, Balzers, Liechtenstein). Images were observed under high vacuum condition at an accelerating voltage of 26 kV.

2.5.2. X-ray diffraction of S-NCs

An X-ray powder diffractometer (Xpert MPD, Philips, Amsterdam, Netherlands) with Cu anode at 40 kV and 20 mA was applied to identify the X-ray diffraction (XRD) patterns of S-NCs. The diffraction angle was 6–50° with a certain step-scan (0.01°) and a count time (2 s per step). The software spectrum viewer (version 2.6) was used to assess the crystallinity level by plotting the peaks baseline on the diffractograms and calculating the percentage of proportion of area under the peaks to total curve area (Jivan et al., 2013).

2.6. Preparation of sour lemon peel extract

The sour lemon peel extract (SLPE) was prepared by an ultrasound-assisted aquoues extraction. 10 g of dried SLP powders was mixed with 10 mL of distilled water and then treated in an ultrasonic bath at 40 kHz and 25 ± 2 °C for 60 min. The resulted aquoues mixture was filtered through a Whatman No. 1 filter paper, concentrated to one-fifth of the initial volume under vacuum at 40 °C using a rotary evaporator (Laborata 4003 model, Heidolph, Schwabach, Germany), and then stored at 4 °C until use.

2.7. Preparation of bioactive coating solutions

Dissimilar concentrations of S-NC (2–10%) and SLPE (2.5–12.5%) were added to the distilled water and then mixed at various amounts of mixing temperature (M-TE, 25–65 °C) and time (M-TI,15–75 min) on a stirrer to prepare the different coating formulations.

2.8. Antioxidant activity of coating solutions

Antioxidant activities of the coating solutions based on S-NC-SLPE were evaluated by the estimation of DPPH-radical scavenging percentage (Ge et al., 2009). The methanolic solution of DPPH (4 mM) was mixed with 50 μL of the each solution by shaking at 150 rpm and then was incubated at 25 °C for 30 min in the dark. The absorbance of solutions was measured using a UV–visible spectrophotometer (Cary 300, Varian Australia, Pty. Ltd.) at 517 nm. The scavenging activity of DPPH · was measured as follows (Eq. (1)):

$$\text{DPPH}^{\cdot}\text{scavenging activity}\ (\%) = ((Ab_0 - (Ab_1/Ab_2))/Ab_0) \times 100 \quad (1)$$

where Ab_0, Ab_1 and Ab_2 are the absorbance amounts of control (without sample), the sample and the sample without DPPH·, respectively.

2.9. Antimicrobial activity of coating solutions

The filter disc diffusion plate was used to determine the antibacterial activity of S-NC-SLPE coating solutions (Rostami and Gharibzahedi, 2017). 100 μL of prepared 0.5 McFarland (Merck, Germany) standard suspensions in MHA (10^6 cells/mL) of each selected bacteria (*S. aureus* PTCC 1189, *E. coli* PTCC 1330, *L. monocytogenes* PTCC 1298, and *S. typhimurium* ATCC 14028) were added to the nutrient medium. A paper disk with a thickness of 1 mm and a diameter of 6 mm, containing 100 μL of S-NC-SLPE coating solutions with different

concentrations was placed in the center of the plate after the top agar had solidified and then plates incubated at 37 °C for 24 h. The diameter (mm) of inhibition zones using a digital vernier caliper was determined as an indicator for the antimicrobial activity. The control was a blank plate containing nutrient agar.

2.10. Colour of coating solutions

The colour changes of S-NC-based edible coating incorporated with SLPE were investigated using a Minolta Chroma Meter CR-200 (Konica Minolta Inc., Tokyo, Japan) in the CIE-L^* a^* b^* scale. The investigated colour parameters were L^* (lightness (+), darkness (−)), a^* (red (+), green (−)), and b^* (yellow (+), blue (−)).

2.11. Viscosity of coating solutions

The viscosity of various coating solutions were determined by a rotational programmable viscometer (LVDV-II Pro, Brookfield Engineering Inc., USA) by using LV spindle according to the method described by Moghaddam et al. (2018). To do that ca. 20 mL of each coating treatments were poured into the viscometer cylinder and shear rate was programmed to increase from 1.6 to 76.6 s^{-1} within 5 s intervals. Flow behavior of coating solutions were determined by fitting the experimentally measured shear stress–shear rate data to the following models: Power law (Eq. (2)), Herschel–Bulkley (Eq. (3)), Bingham (Eq. (4)), and Casson (Eq. (5)) (Garavand and Madadlou, 2014):

$$\tau = k\gamma^n \quad (2)$$

$$\tau = \tau_0 + k\gamma^n \quad (3)$$

$$\tau = \tau_0 + k\gamma \quad (4)$$

$$\tau^{0.5} = \tau_0^{0.5} + k\gamma^{0.5} \quad (5)$$

where, γ is the shear rate (1/s), τ is the shear stress (Pa), K is the consistency index (Pa s^n), n is the flow behavior index (dimensionless), and τ_0 is the yield stress (Pa).

2.12. Response surface optimization

The effective range of the independent variables including S-NC concentration, SLPE incorporation level, M-TE and M-TI to have the best antioxidant and anti-activity of *E. coli* was determined by single-factor-test. Then, these independent variables (S-NC concentration (X_1, 2–10%), SLPE concentration (X_2, 2.5–12.5%), M-TE (X_3, 25–65 °C) and M-TI (X_4, 15–75 min)) during the preparation of edible coatings were optimized by RSM-central composite design (CCD). The Design Expert Version 8.0 (Minneapolis, MN, USA) software designed 30 experimental combinations in a random order at five levels for the each studied parameter (Table 1) to evaluate response variables including antioxidant activity (Y_1), antimicrobial potential against *S. aureus* (Y_2), *E. coli* (Y_3), *L. monocytogenes* (Y_4), and *S. typhimurium* (Y_5), colour parameters of L^* (Y_6), a^* (Y_7), and b^* (Y_8) and viscosity (Y_9). A second-order polynomial equation with the coded independent variables (x_i, $_j$) was studied to (Eq. (6)):

$$Y = \beta_{k0} + \sum_{i=1}^{4} \beta_{ki} x_i + \sum_{i=1}^{4} \beta_{kii} x_i^2 + \sum_{i<j=2}^{4} \beta_{kij} x_i x_j \quad (6)$$

where Y is the response variables (antioxidant, antimicrobial, colour parameters and viscosity); β_{k0}, β_{ki}, β_{kij} and β_{kii} exhibit regression coefficients; and, x_i and x_j show the coded independent parameters.

The coefficient of determination (R^2), adjusted R^2 (R^2_{adj}), the prediction error sum of squares (PRESS), and adequate precision (Ad-P) were applied to determine the adequacy of constructed models (Gharibzahedi et al., 2015a, 2015b; Yousefi et al., 2015). The verification of experimental data under the optimal conditions determined by RSM-CCD was evaluated by performing five additional tests.

2.13. Preparation of coated chicken fillets

Fresh chicken breast fillets were cut into 7 × 15 cm squares of 3 cm of thickness. The coating solutions with different processing and formulation parameters were sprayed through a nozzle on the fillets (50.0 g) and then stored at 4 °C for 12 days. *Quality analyses of chicken fillets.*

2.13.1. Moisture

The moisture content of coated chicken fillets was determined by their drying in an oven at 102 ± 1 °C to constant weight (AOAC, 2005).

2.13.2. Acidity and pH

The titratable acidity of homogenized fillets with distilled water was measured by titration 0.1 N NaOH in the presence of 0.5 mL phenolphthalein was analyzed (AOAC, 2005). A digital pH meter (Metrohm 827 pH lab, Switzerland) was also used to measure the pH after homogenizing 5.0 g of chicken fillet with 50 mL of distilled water.

2.13.3. Thiobarbituric acid reactive substances

The described procedure of Natseba et al. (2005) with slight modifications was used to colourimetrically analyze the thiobarbituric acid reactive substances (TBARS, MDA per kg of the fillet). 200 mg of the both uncoated and coated samples was dissolved with 1.0 mL of 1-butanol into a 25-mL volumetric flask and then diluted to the volume and mixed. After transferring 5 mL of the obtained mixture into a test tube, 5 mL of thiobarbituric acid (TBA) reagent was added, vortexed and placed in a water bath at 95 °C for 120 min. After that, the test tube was cooled up to 25 ± 2 °C and its absorbance was measured by a UV–visible spectrophotometer (Cary 300, Varian Australia, Pty. Ltd.) at 530 nm. Finally, the TBA value was estimated according to the following equation (Eq. (7)):

$$TBA = \left((A_S - A_b) \times 50/200 \right) \quad (7)$$

where A_s and A_b are the absorbance of sample and blank, respectively.

2.13.4. Colour

Three colour parameters of L^*, a^*, and b^* similar with the colour analysis of coating solutions were measured by means of a colour meter instrument (CR-200 model, Konica Minolta Inc., Tokyo, Japan). The total colour difference (ΔE) based on chromaticity coordinates CIE-L^*, a^*, $b^*$was also calculated by the following equation (Eq. (8)):

$$\Delta E = \sqrt{(L_t * - L_{t0})^2 + (b_t * - b_{t0})^2 + (a_t * - a_{t0})^2} \quad (8)$$

where t refers to day 0 and t_0 refers to day 14 (Vatankhah et al., 2017).

2.13.5. Texture

The hardness of chicken fillets was evaluated using a Texture Analyzer TA-XT2i (Stable Micro System, Surrey, UK) equipped with a 50 N load cell and integrator. Samples were axially compressed by a 10 mm-cylindrical probe at a loading speed of 1 mm/s. The maximum force (N) required to compress the sample was determined as the hardness value.

2.13.6. Sensory attributes

The organoleptic analysis of uncoated and coated chicken fillet pieces (3 × 3 cm) in terms of odor/flavor, texture, colour and overall acceptability was performed by 15 trained panelists (6 male and 9 female). Evaluation of the sensory attributed was according to a nine-point hedonic scale so that the scores ranged from 1 (most disliked) to 9

Table 1
The RSM-CCD with studied independent and response variables to optimize the bioactive coating solutions.

Run no.	Independent variables (X_{1-4})					Response variables (Y_{1-9})[a]							
	S-NC (%)	SLPE (%)	M-TE (°C)	M-TI (min)	Viscosity (mPa.s)	Antioxidant activity (%)	Antimicrobial activity (mm)				Colour attributes		
							S. aureus	*E. coli*	*L. monocytogenes*	*S. typhimurium*	Lightness (L^*)	Redness (a^*)	Yellowness (b^*)
1	4	5	35	30	35.11 ± 0.72	88.46 ± 0.92	7.08 ± 0.21	2.46 ± 0.01	3.06 ± 0.05	2.91 ± 0.28	78.13 ± 0.27	3.33 ± 0.54	13.18 ± 0.06
2	8	5	35	30	80.36 ± 0.98	90.80 ± 0.06	6.21 ± 0.03	2.43 ± 0.20	3.59 ± 0.10	2.71 ± 0.14	75.92 ± 0.96	4.45 ± 0.48	15.48 ± 0.14
3	4	10	35	30	39.12 ± 0.66	86.28 ± 0.72	6.04 ± 0.07	3.05 ± 0.11	4.03 ± 0.11	2.89 ± 0.04	73.54 ± 0.59	7.74 ± 0.05	23.48 ± 0.25
4	8	10	35	30	85.22 ± 1.33	90.96 ± 0.21	6.74 ± 0.12	2.70 ± 0.05	3.03 ± 0.04	2.67 ± 0.26	69.97 ± 0.15	9.64 ± 0.32	20.10 ± 0.31
5	4	5	55	30	33.29 ± 0.85	90.46 ± 0.14	2.97 ± 0.06	3.17 ± 0.11	2.30 ± 0.10	2.37 ± 0.26	74.39 ± 1.03	8.71 ± 0.24	15.94 ± 0.15
6	8	5	55	30	79.08 ± 1.71	89.29 ± 0.75	2.66 ± 0.01	2.79 ± 0.10	3.40 ± 0.02	1.92 ± 0.09	71.86 ± 0.85	10.17 ± 0.38	16.46 ± 0.75
7	4	10	55	30	36.11 ± 1.00	87.30 ± 1.12	4.19 ± 0.00	2.99 ± 0.14	2.94 ± 0.09	1.90 ± 0.11	75.44 ± 1.18	9.63 ± 0.21	21.05 ± 0.19
8	8	10	55	30	80.44 ± 1.54	86.62 ± 0.61	5.05 ± 0.04	2.17 ± 0.06	2.45 ± 0.04	1.76 ± 0.38	65.66 ± 1.39	13.04 ± 0.16	17.20 ± 0.30
9	4	5	35	60	38.58 ± 0.62	87.30 ± 0.24	7.68 ± 0.11	2.17 ± 0.06	2.74 ± 0.05	2.01 ± 0.46	80.96 ± 0.05	4.81 ± 0.50	13.48 ± 0.05
10	8	5	35	60	82.20 ± 0.98	81.77 ± 0.09	4.93 ± 0.18	2.72 ± 0.11	2.90 ± 0.04	2.13 ± 0.27	78.97 ± 0.41	5.83 ± 0.16	11.98 ± 0.45
11	4	10	35	60	39.37 ± 0.44	88.79 ± 0.04	4.27 ± 0.21	2.64 ± 0.10	4.08 ± 0.03	2.14 ± 0.25	78.34 ± 0.08	6.67 ± 0.06	19.62 ± 0.24
12	8	10	35	60	89.49 ± 1.88	85.96 ± 0.71	3.80 ± 0.10	2.48 ± 0.14	3.09 ± 0.11	2.11 ± 0.20	73.56 ± 0.42	10.52 ± 0.14	16.60 ± 0.18
13	4	5	55	60	30.69 ± 0.35	90.13 ± 0.21	4.05 ± 0.02	3.35 ± 0.18	2.72 ± 0.09	2.20 ± 0.41	76.05 ± 0.62	8.77 ± 0.45	13.29 ± 0.15
14	8	5	55	60	72.20 ± 0.90	82.13 ± 0.63	3.35 ± 0.02	3.90 ± 0.10	3.28 ± 0.09	2.20 ± 0.02	70.03 ± 0.85	15.24 ± 1.02	13.99 ± 0.15
15	4	10	55	60	29.97 ± 0.65	91.97 ± 1.05	4.70 ± 0.02	3.43 ± 0.23	3.41 ± 0.10	1.81 ± 0.20	75.46 ± 0.48	10.08 ± 0.25	19.23 ± 0.02
16	8	10	55	60	95.15 ± 1.93	82.44 ± 0.19	5.00 ± 0.15	2.66 ± 0.11	2.94 ± 0.00	2.02 ± 0.14	69.64 ± 1.04	11.14 ± 0.41	11.63 ± 0.07
17	2	7.5	45	45	52.02 ± 0.75	93.42 ± 2.16	3.55 ± 0.19	3.44 ± 0.05	3.07 ± 0.08	3.80 ± 0.11	82.73 ± 1.11	4.01 ± 0.15	16.04 ± 0.41
18	10	7.5	45	45	58.88 ± 1.00	88.46 ± 1.05	3.21 ± 0.07	3.44 ± 0.18	3.07 ± 0.01	3.39 ± 0.20	74.52 ± 0.04	6.54 ± 0.61	11.14 ± 0.24
19	6	2.5	45	45	62.07 ± 0.79	83.44 ± 0.41	5.13 ± 0.01	2.97 ± 0.19	2.61 ± 0.01	3.18 ± 0.09	80.37 ± 0.66	3.97 ± 0.11	10.45 ± 0.07
20	6	12.5	45	45	50.94 ± 0.65	84.94 ± 0.29	5.20 ± 0.03	2.37 ± 0.06	3.05 ± 0.05	3.18 ± 0.00	73.05 ± 0.72	10.64 ± 0.41	19.84 ± 0.06
21	6	7.5	25	45	55.52 ± 0.39	82.44 ± 0.15	6.25 ± 0.01	0.91 ± 0.26	3.30 ± 0.17	1.82 ± 0.15	71.53 ± 0.04	8.59 ± 0.09	15.25 ± 0.30
22	6	7.5	65	45	54.05 ± 0.81	81.77 ± 0.33	2.24 ± 0.02	1.27 ± 0.13	2.93 ± 0.10	0.83 ± 0.06	61.87 ± 0.98	61.87 ± 0.88	12.48 ± 0.13
23	6	7.5	45	15	58.11 ± 0.91	89.45 ± 0.27	7.47 ± 0.02	4.25 ± 0.05	3.17 ± 0.07	1.39 ± 0.07	75.24 ± 0.31	6.30 ± 0.14	21.55 ± 0.14
24	6	7.5	45	75	55.19 ± 0.57	85.61 ± 0.48	6.86 ± 0.09	4.70 ± 0.08	3.38 ± 0.00	0.43 ± 0.00	78.68 ± 0.70	8.52 ± 0.09	16.04 ± 0.35
25	6	7.5	45	45	58.62 ± 0.80	85.11 ± 0.51	4.15 ± 0.14	2.92 ± 0.19	2.54 ± 0.05	1.53 ± 0.05	76.74 ± 0.01	7.78 ± 0.02	16.13 ± 0.41
26	6	7.5	45	45	55.58 ± 0.64	87.95 ± 0.06	4.57 ± 0.05	3.15 ± 0.04	2.50 ± 0.01	1.42 ± 0.01	77.42 ± 0.13	4.85 ± 0.13	12.97 ± 0.12
27	6	7.5	45	45	58.78 ± 0.77	84.30 ± 0.68	4.51 ± 0.06	3.09 ± 0.00	2.51 ± 0.02	1.39 ± 0.02	77.61 ± 0.55	6.54 ± 0.05	13.11 ± 0.36
28	6	7.5	45	45	51.58 ± 0.59	85.40 ± 0.32	4.62 ± 0.17	3.21 ± 0.10	2.54 ± 0.05	1.44 ± 0.05	76.82 ± 0.71	5.89 ± 0.31	13.71 ± 0.21
29	6	7.5	45	45	50.80 ± 0.66	86.10 ± 0.19	4.44 ± 0.01	3.16 ± 0.05	2.36 ± 0.12	1.48 ± 0.12	77.31 ± 0.06	7.32 ± 0.14	14.62 ± 0.20
30	6	7.5	45	45	54.23 ± 0.29	85.70 ± 0.15	4.41 ± 0.04	3.11 ± 0.01	2.45 ± 0.03	1.39 ± 0.03	75.32 ± 0.12	6.57 ± 0.26	12.32 ± 0.01

[a] Mean ± standard deviation (n = 2).

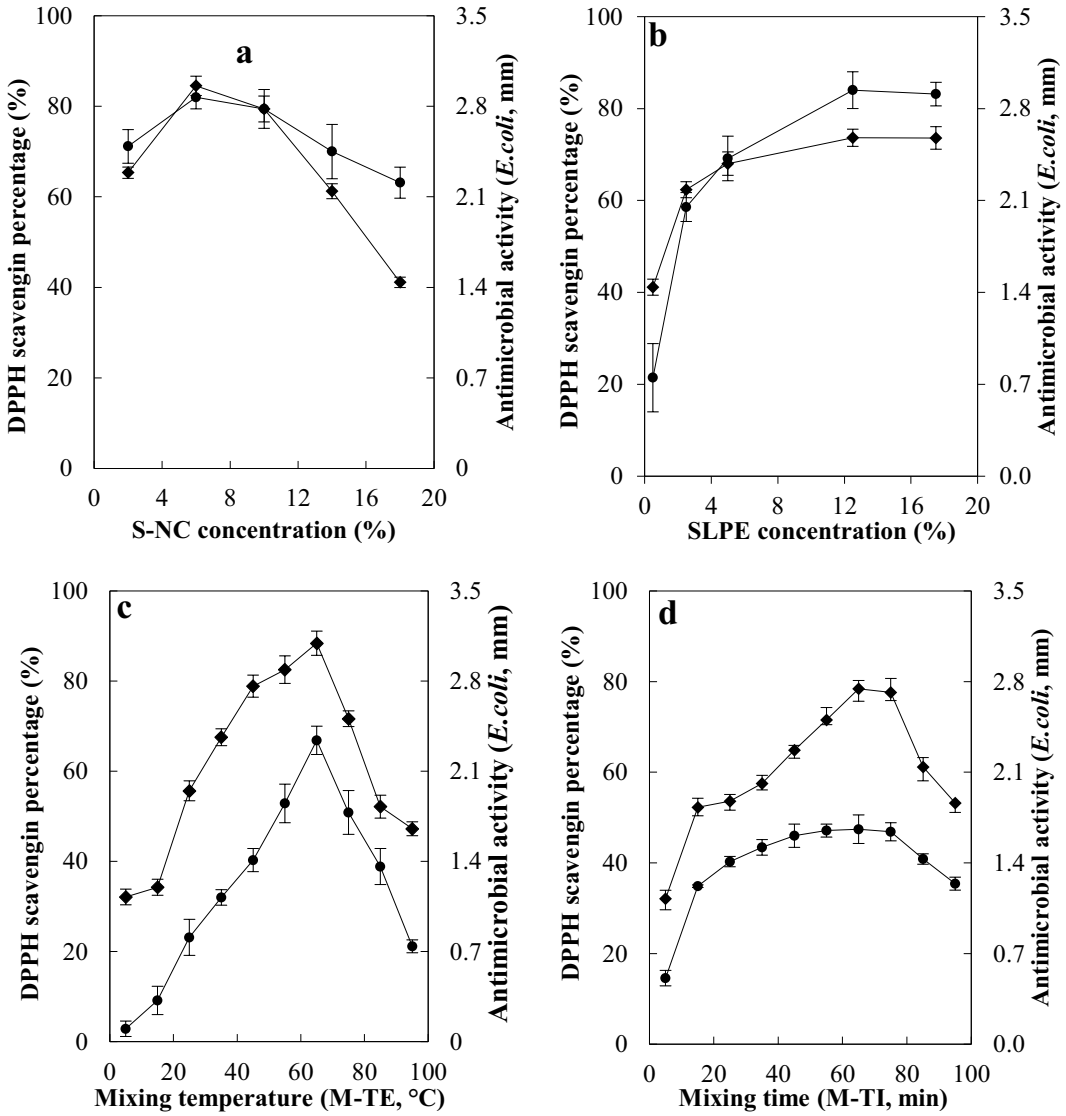

Fig. 1. Effect of different levels of S-NC concentration (a), SLPE incorporation level (b), M-TE (c) and M-TI (d) on the antioxidant activity and anti-activity of *E. coli*.

(most liked).

2.14. Statistical analysis

All experiments were carried out in three replicates and results represented as mean ± standard deviation. Analysis of variance (ANOVA) and Duncan's multiple comparison tests at 95% significance for quality parameters of the uncoated (control, UCCFs) and coated (CCFs) chicken fillets were performed using SPSS software (version 22, SPSS Inc., Chicago, USA).

3. Results and discussion

3.1. Preliminarily studies

The effect of different concentrations of S-NC (2, 6, 10, 14 and 18%) in coating solutions to attain the maximum DPPH· scavenging capacity and anti-activity potential of *E. coli* PTCC 1330 was studied (Fig. 1a). The SLPE incorporation level, M-TE and M-TI were fixed at 10%, 50 °C and 50 min, respectively. An increase in S-NCs level up to 6% led to a maximum level in the antioxidant and antibacterial activities. An insignificant decrease in amounts of these parameters was also observed at 10% S-NC. However, a sharp decline in DPPH· inhibition percentage and *E. coli* PTCC 1330 inactivity was found at S-NC concentrations between 14 and 18% ($p < 0.05$). Therefore, 10% S-NC was adopted in the present study. Improving the antiradical activity of coating solutions by increasing S-NCs by 10% may be related to their emulsifying potential. 10% SLPE contains considerable amounts of essential oils which can convert coating solutions to a bipolar system. Use of 10% S-NCs can suitably stabilize the oil-in-water Pickering emulsion with homogenous and small particles (Li et al., 2014). Two anti-oxidative mechanisms for S-NCs can be expected: (i) inhibition of the diffusion of prooxidants (oxygen and metals like iron) by increasing the viscosity of aqueous phase. This fact decreases the lipid oxidation rate by postponing the oil droplets movement. (ii) S-NC is a strong barrier against the prooxidants diffusion at the interface of oil and water which can significantly reduce the lipid oxidation process (Gharibzahedi et al., 2012). Reducing the antioxidant activity at S-NC levels >10% is probably due to the decrease of the emulsion stability and adsorption area at the interface as a result of excessive aggregates of S-NCs in a highly viscous environment (Li et al., 2012). The high physicochemical stability of Pickering emulsions stabilized with 10% S-NC improved the effectiveness and availability of essential oils to inactive the foodborne pathogen of *E. coli* PTCC 1330.

The inhibition rate of oxidation process and *E. coli* PTCC 1330 growth by coating solutions was improved with increasing

Table 2
ANOVA table for the second-order polynomial models constructed for each the studied response variable.

Source	DF	Antioxidant activity (%)				Viscosity (mPa·s)				Antimicrobial activity of *E. coli* (mm)			
		SS	MS	F-value	P-value	SS	MS	F-value	P-value	SS	MS	F-value	P-value
Model	14	271.73	19.41	13.56	< 0.0001	11,235.0	802.498	65.71	0.000	15.84	1.13	36.28	<0.0001
X_1 (S-NC)	1	39.12	39.12	27.32	0.0001	49.3	49.316	4.04	0.063	0.08	0.08	2.66	ns
X_2 (SLPE)	1	0.37	0.37	0.26	ns	0.2	0.213	0.02	0.897	0.18	0.18	5.73	0.0302
X_3 (M-TE)	1	0.07	0.07	0.05	ns	0.0	0.039	0.00	0.956	0.86	0.86	27.42	0.0001
X_4(M-TI)	1	31.19	31.19	21.78	0.0003	15.3	15.340	1.26	0.280	0.26	0.26	8.28	0.0115
X_1^2	1	63.37	63.37	44.26	< 0.0001	51.4	51.387	4.21	0.058	0.12	0.12	3.92	ns
X_2^2	1	0.77	0.77	0.54	ns	6.4	6.352	0.52	0.482	0.43	0.43	13.90	0.0020
X_3^2	1	13.01	13.01	9.09	0.0087	13.7	13.681	1.12	0.307	7.44	7.44	238.50	<0.0001
X_4^2	1	12.22	12.22	8.53	0.0105	4.0	3.987	0.33	0.576	2.91	2.91	93.20	<0.0001
X_{12}	1	1.00	1.00	0.70	ns	4.4	4.410	0.36	0.557	0.49	0.49	15.60	0.0013
X_{13}	1	20.34	20.34	14.21	0.0019	3.4	3.422	0.28	0.604	0.13	0.13	4.10	ns
X_{14}	1	60.30	60.30	42.11	< 0.0001	0.0	0.023	0.00	0.966	0.19	0.19	6.14	0.0256
X_{23}	1	3.37	3.37	2.35	ns	8.7	8.702	0.71	0.412	0.58	0.58	18.64	0.0006
X_{24}	1	15.37	15.37	10.73	0.0051	0.6	0.562	0.05	0.833	0.06	0.06	1.96	ns
X_{34}	1	2.02	2.02	1.41	ns	74.0	73.960	6.06	0.026	0.51	0.51	16.28	0.0011
Residual	15	21.48	1.43			183.2	12.212			0.47	0.03		
Lack of fit	10	13.88	1.39	0.91	0.5798^{ns}	121.2	12.123	0.98	0.546^{ns}	0.42	0.04	4.13	0.0655^{ns}
Pure error	5	7.60	1.52			62.0	12.391			0.05	0.01		
Core total	29	293.21				11,418.2				16.31			

Source	DF	Antimicrobial activity of *S. typhimurium* (mm)				Antimicrobial activity of *S. aureus* (mm)				Antimicrobial activity of L. *monocytogenes* (mm)			
		SS	MS	F-value	P-value	SS	MS	F-value	P-value	SS	MS	F-value	P-value
Model	14	16.69	1.19	123.19	< 0.0001	57.09	4.08	48.19	< 0.0001	5.82	0.42	35.44	< 0.0001
X_1	1	0.09	0.09	10.08	0.0063	0.64	0.64	7.57	0.0149	0.01	0.01	1.28	ns
X_2	1	0.05	0.05	5.69	0.0306	0.04	0.04	0.49	ns	0.34	0.34	29.05	< 0.0001
X_3	1	1.20	1.20	124.16	< 0.0001	21.66	21.66	255.95	< 0.0001	0.61	0.61	51.82	< 0.0001
X_4	1	0.82	0.82	84.50	< 0.0001	0.80	0.80	9.45	0.0077	0.02	0.02	2.16	ns
X_1^2	1	7.86	7.86	812.21	< 0.0001	2.13	2.13	25.22	0.0002	0.66	0.66	56.16	< 0.0001
X_2^2	1	5.11	5.11	527.89	< 0.0001	0.77	0.77	9.07	0.0088	0.25	0.25	21.10	0.0004
X_3^2	1	0.03	0.03	2.94	ns	0.11	0.11	1.27	ns	0.76	0.76	64.61	< 0.0001
X_4^2	1	0.51	0.51	52.38	< 0.0001	12.21	12.21	144.32	< 0.0001	1.17	1.17	99.44	< 0.0001
X_{12}	1	0.007	0.007	0.79	ns	2.27	2.27	26.77	0.0001	1.76	1.76	149.62	< 0.0001
X_{13}	1	0.0001	0.0001	0.01	ns	0.78	0.78	9.26	0.0082	0.25	0.25	21.31	0.0003
X_{14}	1	0.11	0.11	11.08	0.0046	1.00	1.00	11.82	0.0037	0.05	0.05	4.12	ns
X_{23}	1	0.09	0.09	10.09	0.0063	7.51	7.51	88.72	< 0.0001	0.23	0.23	19.23	0.0005
X_{24}	1	0.003	0.003	0.34	ns	1.78	1.78	21.06	0.0004	0.20	0.20	16.88	0.0009
X_{34}	1	0.59	0.59	60.87	< 0.0001	3.63	3.63	42.88	< 0.0001	0.29	0.29	24.85	0.0002
Residual	15	0.15	0.009			1.27	0.08			0.18	0.01		
Lack of fit	10	0.13	0.01	4.31	0.0602^{ns}	1.13	0.11	4.08	0.0670^{ns}	0.15	0.01	3.21	0.1051^{ns}
Pure error	5	0.01	0.003			0.14	0.03			0.02	0.004		
Core total	29	16.83				58.36				6.00			

(*continued on next page*)

Table 2 (*continued*)

Source	DF	Lightness (L^*-value)				Redness (a^*-value)				Yellowness (b^*-value)			
		SS	MS	F-value	P-value	SS	MS	F-value	P-value	SS	MS	F-value	P-value
Model	14	554.58	39.61	38.98	< 0.0001	326.16	23.30	15.34	< 0.0001	308.82	22.06	14.42	< 0.0001
X_1	1	117.57	117.57	115.69	< 0.0001	26.78	26.78	17.63	0.0008	27.38	27.38	17.89	0.0007
X_2	1	64.48	64.48	63.45	< 0.0001	38.74	38.74	25.50	0.0001	121.04	121.04	79.11	< 0.0001
X_3	1	104.92	104.92	103.24	< 0.0001	126.27	126.27	83.13	< 0.0001	4.75	4.75	3.11	ns
X_4	1	26.00	26.00	25.58	0.0001	4.85	4.85	3.19	ns	48.45	48.45	31.66	< 0.0001
X_1^2	1	3.45	3.45	3.40	ns	1.86	1.86	1.23	ns	0.42	0.42	0.27	ns
X_2^2	1	0.42	0.42	0.41	ns	1.67	1.67	1.10	ns	7.20	7.20	4.70	0.0466
X_3^2	1	189.21	189.21	186.18	< 0.0001	98.70	98.70	64.98	0.0001	1.01	1.01	0.66	ns
X_4^2	1	0.10	0.10	0.10	ns	2.05	2.05	1.35	ns	55.68	55.68	36.39	< 0.0001
X_{12}	1	7.84	7.84	7.71	0.0141	0.001	0.001	0.0009	ns	24.67	24.67	16.12	0.0011
X_{13}	1	8.41	8.41	8.28	0.0115	1.27	1.27	0.84	ns	1.34	1.34	0.87	ns
X_{14}	1	0.01	0.01	0.01	ns	1.27	1.27	0.84	0.0077	3.07	3.07	2.01	ns
X_{23}	1	9.67	9.67	9.52	0.0075	14.35	14.35	9.44	ns	16.52	16.52	10.80	0.0050
X_{24}	1	2.79	2.79	2.74	ns	5.80	5.80	3.82	ns	2.59	2.59	1.69	ns
X_{34}	1	6.81	6.81	6.70	0.0205	0.06	0.06	0.04		0.24	0.24	0.15	ns
Residual	15	15.24	1.02			22.79	1.52			22.95	1.53		
Lack of fit	10	11.78	1.18	1.70	0.2905[ns]	17.37	1.74	1.61	0.3136[ns]	13.49	1.35	0.71	0.3136[ns]
Pure error	5	3.47	0.69			5.41	1.08			9.46	1.89		
Core total	29	569.83				348.95				331.77			

incorporation level of SLPE from 0.5 to 12.5% at a fixed condition of 10% S-NC, 50 °C M-TE and 50 min M-TI (Fig. 1b) Although the lowest response amounts were detected at 0.5% SLPE, a steep decrease in DPPH· scavenging capacity and *E. coli* PTCC 1330 inactivity was observed at SLPE levels >12.5% (Fig. 1b). There are a high number of bioactive components in the peel of citrus fruits such as essential oils, flavonoids and phenolic acids. Furthermore, the presence of these antioxidant and antimicrobial compounds especially phenolics and essential oils at high concentrations in citrus peel and seed extracts has been proved (Bocco et al., 1998). Therefore, the partition of hydrophobic essential oils in the lipid phase and hydrophilic phenolics in the water phase not only can efficiently quench oxidative free radicals, but also can accelerate the diffusion into the membrane of bacterial cells to leakage of their cell contents (Burt, 2004; Gharibzahedi and Mohammadnabi, 2016).

The effect of various M-TE levels (5–95 °C, with an interval of 10 °C) on the bioactivity of coating solutions was depicted in Fig. 1c, when the other parameters including S-NC and SLPE concentrations, and M-TI were fixed at 10%, 12.5% and 50 min, respectively. With the exception of two studied initial temperatures (5 and 15 °C), a significant increase in the antioxidant and antibacterial activities of coating solutions was observed in the M-TE range of 15–65 °C ($p < 0.05$; Fig. 1c). An increase in M-TE can lead to a higher mobility of S-NCs for crosslinking with phenolics of SLPE and may accordingly form a high number of small phenolic aggregates at the interface of antioxidant essential oils-in-water emulsions. Increasing the diffusion coefficient of bioactive compounds and their movement towards membrane of bacterial cells at high temperatures can destroy the microbial cells via their interaction with proteins present in the cytoplasmic membrane (Nychas et al., 2003). The steep drop in bioactivity of coating solutions at M-TE >65 °C (Fig. 1c) probably is due to the hydrolysis and structural destruction of phenolic acids and flavonoids. In addition, reducing the viscosity amount at high temperatures leads to an increase in coalescence rate of the formed emulsion (Xu et al., 2008). Under this condition, the lipoxygenase and free radicals easily penetrate into the lipid phase to increase the oxidation rate (Gharibzahedi et al., 2012).

The antioxidant activity and inhibition level of *E. coli* PTCC 1330 were increased with an increase in M-TI from 15 to 75 min at a fixed condition including 10% S-NC, 12.5% SLPE, 65 °C M-TE. A high bioactivity for coating solutions could not be supported by applying 15 min ≤ M-TI ≤ 75 min. An increase in M-TI by 75 min provides an ideal opportunity to form the antioxidant complexes between S-NC and SLPE, whereas the more increase by 95 min reduced the bioactivity of biopolymeric solution possibly due to the degradation of phenolic and flavonoid components (Xu et al., 2008).

3.2. Fitness assessment of RSM models

Second-order polynomial models ($p < 0.0001$) with non-significant lack-of-fit values ($p > 0.05$) were fitted to the experimental data. The high R^2 (0.926–0.991) and R^2_{adj} (0.858–0.983) values with low PRESS (0.77–107.87) amounts demonstrate the adequacy of fitted quadratic equations. Since a high R^2 value cannot always explain the fitness of regression models, there is a modified form of R^2 namely R^2_{adj} that regulates for the number of explanatory terms in a constructed model. R^2_{adj} in comparison with R^2 escalates only if the new term develops the model better than would be expected by chance (Gharibzahedi, 2017). The Ad-P determines the signal-to-noise ratio, so that a ratio >4.0 would be appropriate (Yousefi et al., 2015). The Ad-*P* values for fitted models with the experimental data of DPPH· inhibition rate (15.81), antibacterial activity against *S. aureus* (20.16), *E. coli* (31.79), *L. monocytogenes* (21.46) and *S. typhimurium* (45.74), colour L^* (28.80), a^* (18.36) and b^* (13.36) and viscosity (44.98) values show that these models are able to navigate the design space.

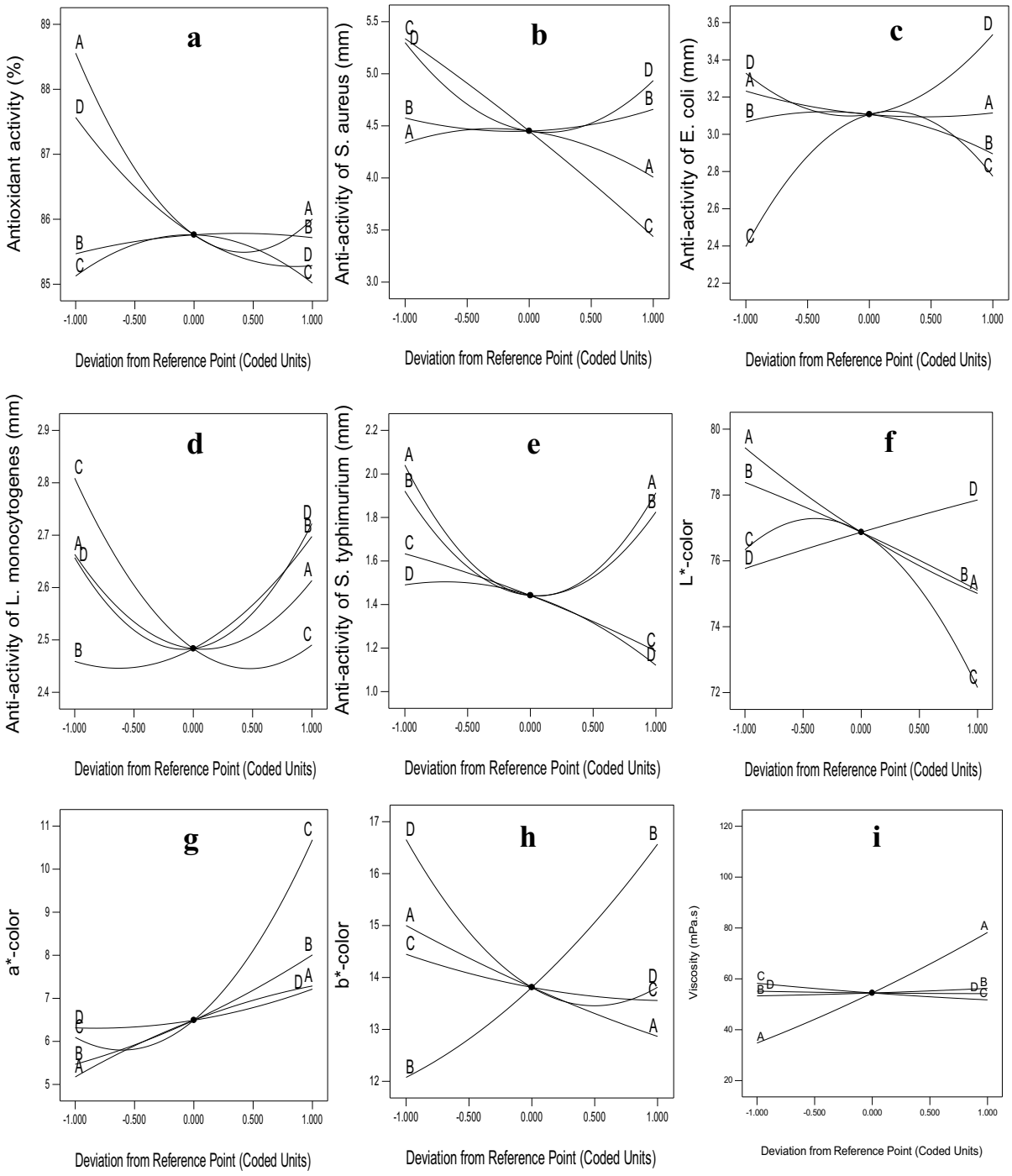

Fig. 2. Perturbation graphs showing the effect of independent variables on DPPH· scavenging percentage (b), antibacterial activities against *S. aureus* (b), *E. coli* (c), *L. monocytogenes* (d) and *S. typhimurium* (e), colour L^* (f), a^* (g), and b^*(h) and viscosity (i) values of preservative coating solutions (Actual factors: A, S-NC: 6.0%; B, SLPE: 7.5%; C, M-TE: 45 °C; D, M-TI: 45 min).

3.3. Antioxidant activity optimization of coating solutions

Table 2 reveals that the linear terms of S-NC concentration and M-TI were significant on the DPPH· scavenging rate ($p = 0.0001$; $p < 0.001$). Among the quadratic terms, the only effect of SLPE was insignificant. Three interaction terms of S-NC concentration and M-TE ($p < 0.01$), S-NC amount and M-TI ($p < 0.0001$), and SLPE incorporation level and M-TI ($p < 0.01$) were significant on the antioxidant activity. Fig. 2a shows an increase in SLPE level incorporated into coating solutions can increase the antiradical scavenging activity, while increasing levels of other independent variables led to a decrease in the antioxidant activity. The interaction and linear terms of S-NC concentration and M-TI were the most significant parameters on antioxidant activity of the coating solutions. The highest DPPH· inhibition percentage (91.05%) was obtained under the experimental conditions of 4% S-NC, 10% SLPE, 52.14 °C M-TE and 59.99 min M-TI. The effect of S-NCs concentration on the antioxidant activity can be justified by the physical stability of developed Pickering emulsions. Presence of an

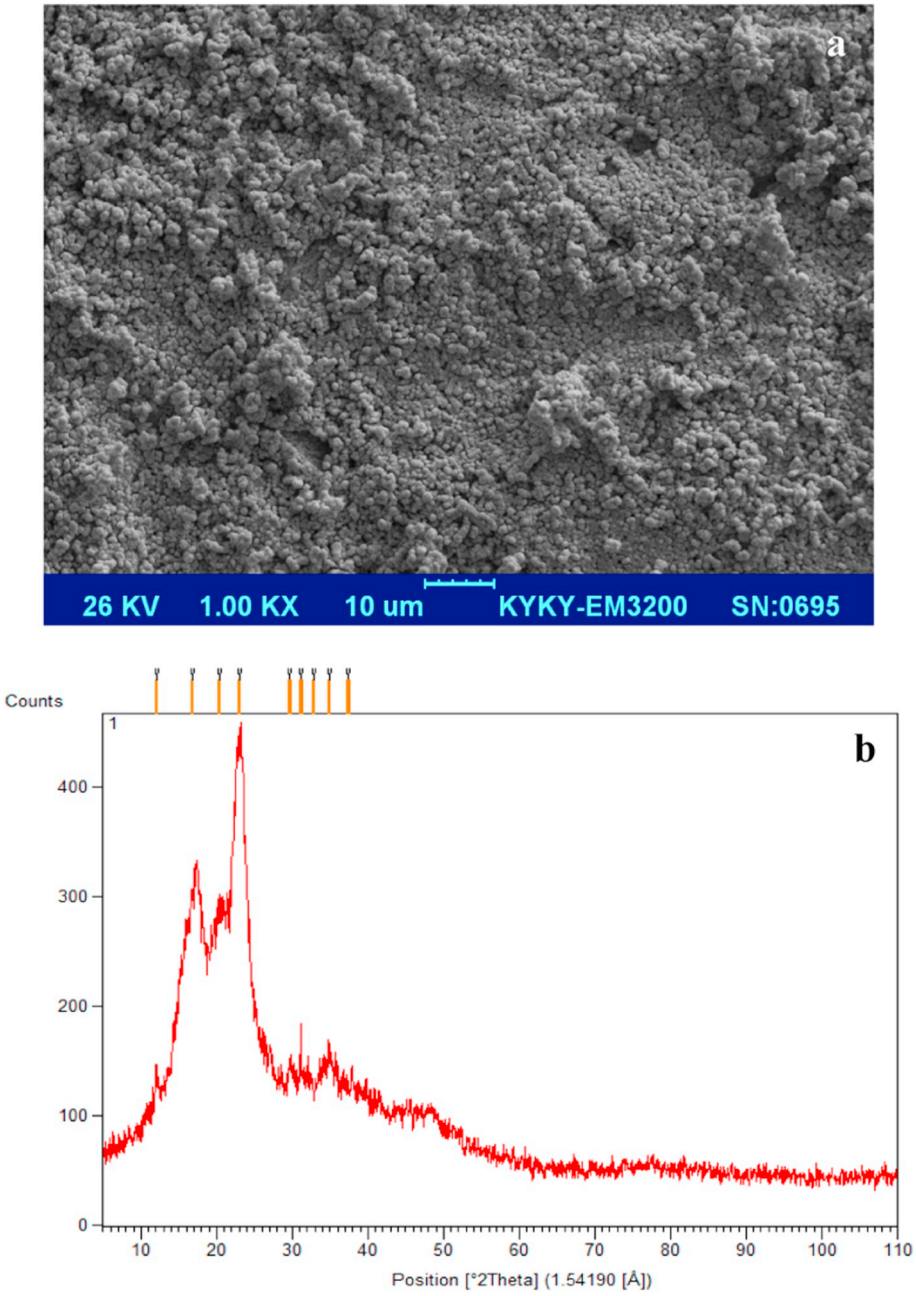

Fig. 3. Scanning electron micrograph (a) and X-ray diffraction patterns (b) of the S-NCs.

emulsion gel structure because of the aggregated network formation of S-NC-bridged droplets can efficiently prevent the lipid oxidation by decelerating the prooxidants mobility in the continuous phase (Li et al., 2012). Moreover, the complete surface coverage/adsorption of oil droplets by 4% S-NC not only can improve the droplets stability against aggregation or coalescence, but also can inhibit the lipid oxidation process (Kargar et al., 2012). Reducing the oxidative stability of coating solutions at concentrations >4.0% S-NC may be related to their considerable reduction of emulsion droplets size (Lethuaut et al., 2002). The larger specific surface area for many numbers of small S-NCs (~ 150 nm) with the dominant crystalline nature (Fig. 3a and b) can significantly increase the oxidation rate. The longer exposure time of essential oils emulsified in the aquoues phase with low viscosity at high M-TE probably increase the lipid oxidation through the activity of lipoxygenase and free radicals and degradation of phenolics and flavonoids of SLPE present in the system (Gharibzahedi et al., 2012; Xu et al., 2008).

3.4. Antimicrobial capacity optimization of coating solutions

There is a discrepancy in ANOVA results for the antimicrobial activity of coating solutions against the studied four bacteria. The linear effect of S-NC on the growth inhibition of *E. coli* PTCC 1330 and L. *monocytogenes* PTCC 1298 was non-significant (Table 2), while a significant main effect for S-NC was found for the antimicrobial activities of *S. aureus* PTCC 1189 ($p < 0.05$) and *S. typhimurium* ATCC 14028 ($p < 0.01$). The linear effect of SLPE on the growth inhibition of all bacteria except *S. aureus* PTCC 1189 was significant (Table 2). In addition, the significant main effects of M-TE and M-TI on the inactivation of all the studied bacteria with the exception of L. *monocytogenes* PTCC 1298 were observed. Although the linear effect of M-TE was significant on the anti-activity of L. *monocytogenes* PTCC 1298, the linear term of M-TI on this bacterium was ineffective (Table 2). The interaction effects of all the independent variables were significant on the inhabitation rate of *S. aureus* PTCC 1189. Two interaction terms of S-NC/M-TE and

SLPE/M-TI were not significant on the inactivation of *E. coli* PTCC 1330 and *S. typhimurium* ATCC 14028. In addition, the interaction effects of S-NC/SLPE and S-NC/M-TI were insignificant on *S. typhimurium* ATCC 14028 and *L. monocytogenes* PTCC 1298, respectively. Moreover, the effects of independent variables on the antimicrobial activity as depicted in perturbation graphs demonstrate that S-NC significantly reduced this parameter (Fig. 2b-e). The most significant effect on the inactivation changes of *S. aureus* PTCC 1189, *E. coli* PTCC 1330, *L. monocytogenes* PTCC 1298, and *S. typhimurium* ATCC 14028 were the linear effect of M-TE, the quadratic effect of M-TE, the interaction effect of S-NC/SLPE and the quadratic effect of S-NC, respectively. The individual optimum condition showed that the highest antimicrobial activities against *S. aureus* PTCC 1189 (6.05 mm), *L. monocytogenes* PTCC 1298 (3.92 mm), *E. coli* PTCC 1330 (3.15 mm), and *S. typhimurium* ATCC 14028 (2.97 mm) would be obtained at 4% S-NC, 10% SLPE, 35 °C M-TE and 30 min M-TI.

Overall, Gram-negative bacteria (e.g., *E. coli* and *S. typhimurium*) against the antimicrobial agents because of the having an additional exterior membrane with highly hydrophilic surfaces possess a more resistance than Gram-negative ones (e.g., *S. aureus* and L. *monocytogenes*). However, the presence of water-insoluble residues of lipoteichoic acids in the cell membrane of Gram-positive bacteria intensifies the penetration rate by non-polar components (Gharibzahedi and Mohammadnabi, 2016). The microbial growth inhibition effect of S-NC may be ascribed to the decrease of surface and interfacial tension of droplets and thus the increase of adsorption rate of phenolics and flavonoids present in SLPE on the membrane of bacterial cells (Kurup et al., 1991). Although an increase in M-TE can improve the diffusion rate of bioactive compounds towards the membrane of microorganisms, much more M-TEs may reduce the antimicrobial activity of coating solutions with the structural damage of heat-labile bioactive constituents of SLPE (Xu et al., 2008).

3.5. Colour parameters optimization of coating solutions

As clearly illustrated in Table 2, the linear terms of S-NC and SLPE had a significant effect on the colour L^*, a^* and b^* values of coating solutions ($p \leq 0.0001$; $p < 0.001$). However, only the linear effect of M-TE on the yellowness and the linear effect of M-TI on the redness were not significant (Table 2). The quadratic effects of independent variable on the colour parameters were mostly insignificant. The significance of cross terms on the lightness (S-NC/SLPE; S-NC/M-TE; SLPE/M-TE; M-TE/M-TI), redness (S-NC/M-TI) and yellowness (S-NC/SLPE; SLPE/M-TE) was also studied (Table 2). Fig. 2f-h also reveals that an increase in M-TI, M-TE and SLPE respectively led to a significant increase in the colour L^*, a^* and b^* values. According to the sum of squares, the importance of the independent variables on the lightness of coating solutions could be ranked in the following order: S-NC > M-TE > SLPE. However, the optimization technique proved that the lowest colour a^* (3.32) and b^* (11.54) values and the highest colour L^* value (80.91) were obtained when the coating solutions was formulated with 4% S-NC and 5% SLPE at 38.53 °C M-TE and 50.26 min M-TI.

Colour is considered as a key parameter for edible coating solutions in terms of appearance and the consumer acceptance of final coated products. High concentrations S-NCs probably due to the formation of large aggregates with the high water-holding potential and strong interactions with other hydrophilic components in coating solutions can significantly reduce the lightness value (Viguie et al., 2007). Increasing the redness of coating solutions at high M-TI levels may be explained by two phenomena including (i) the heating hydrolysis of phenolics and high number of degraded products in the environment and (ii) the enhanced quantity of interactions between SLPE and S-NCs due to the more molecular mobility and lower viscosity of the fluid. However, it seems that a good dispersion of SLPE in the S-NCs matrix at longer M-TIs can lead to a more lightness due to the suitable chemical affinity between both components (Condés et al., 2015). Increasing the yellowness of coating solutions at high SLPE concentrations also is related to the natural pale yellow colour of essential oils (Burt, 2004).

3.6. Viscosity optimization of coating solutions

Determination of the viscosity of coating solutions containing nanocrystal suspensions is important in designing of suitable coatings for food items and delivery of active components as affected by thermal and transportation conditions (Jiang et al., 2016; Garavand et al., 2017). As showed in Table 2 the both linear and quadratic terms of S-NC concentration, SLPE concentration, MT-E and M-TI were significant on the viscosity of the prepared coatings ($p < 0.001$). The interaction terms of all studied variables were also significant on the viscosity. Fig. 2i demonstrated that increase in S-NC concentration into the coating solutions can increase the viscosity considerably, while elevated amounts of SLPE, MT-E and M-TI caused a slight drop in viscosity of coating solutions. Under the following experimental data the minimum viscosity (22.4 mPa.s) of coating solutions was acquired: 2% S-NC, 7.5% SLPE, 45 °C M-TE and 45 min M-TI. All of the investigated coating solutions were followed a shear-thinning behavior and well-fitted by power law model. Le Corre (2011) was also reported similar rheological trends for waxy maize starch nanocrystals at the concentrations of 5–10%. S-NC can absorb water from suspension and generate a viscous medium based on the deformation of the swollen starch granules and the volume ratio of dispersed phase and dispersion medium (Lin et al., 2011a, 2011b). Zhang et al. (2010) reported that higher concentrations of S-NC in suspensions can affect the rheological attributes and generate high-viscous or gelation with is not desirable for constructing films and coatings.

3.7. Overall optimization and verification studies

The simultaneous numerical optimization of multiple responses with the target of maximum antioxidant and antimicrobial activities and lightness intensity and also the lowest redness and yellowness colour values were carried out. Results showed that the combination of 4.0% S-NC and 5.62% SLPE in an aquoues solution treated at 51.17 °C for 43.29 min can provide the desirable targets. The corresponding predicted response values for the DPPH· inhibition percentage, antimicrobial capacities against *S. aureus*, *E. coli*, *L. monocytogenes* and *S. typhimurium* and colour attributes of lightness, redness, yellowness and viscosity were 89.14%, 3.58 mm, 3.14 mm, 2.31 mm, 2.24 mm, 77.82, 6.69, 13.21 and 27.5 mPa.s, respectively. Five additional tests under the determined optimal conditions for the preparation of coating solutions were performed to check the reliability of the developed quadratic models. The experimental data for the DPPH· scavenging rate, antimicrobial activities against *S. aureus*, *E. coli*, *L. monocytogenes* and *S. typhimurium*, colour attributes of lightness, redness and yellowness and viscosity under the optimal conditions were 88.24 ± 1.79%, 3.62 ± 0.12 mm, 3.14 ± 0.07 mm, 2.31 ± 0.07 mm, 2.19 ± 0.05 mm, 75.93 ± 1.65, 6.60 ± 0.14, 12.54 ± 0.76, and 26.96 ± 0.88 mPa.s, respectively. The closeness between the experimental and predicted response values ($p > 0.05$) demonstrates adequacy of the fitted quadratic models.

3.8. Storage qualities of chicken fillets coated with the optimal solution

Table 3 shows the mean values for physical (moisture and colour attributes), chemical (acidity and TBARS), textural (hardness), and sensory (odor/flavor, texture, colour and overall acceptability) properties of the CCFs and UCCFs at the initial (1st) and final (12th) storage days. Table 3 also represents the best regression relationships between these quality characteristics and storage time and their R^2 values. In general, the CCFs had a better quality characteristics compared to the UCCFs, so that the quality deterioration rate in CCFs was much slower than that of in CCFs ($p < 0.05$). There were no significant differences at the 1st storage day between CCFs and UCCFs in amounts of moisture, acidity,

Table 3
Quality changes of physicochemical, textural, colour and sensorial parameters of chicken fillets during the cold-storage time.

Quality properties[a]	Values at the initial and end storage time[b]		Change (%)[c]	The best fitted regression equation[d]	R^2
	Day 1	Day 12			
Moisture (%)					
CCFs	66.23 ± 0.14[a]	68.15 ± 0.08[a]	2.89[a]	$Y = 0.0586\ ST^2 - 0.5871\ ST + 66.759$	1.000
UCCFs	66.55 ± 0.26[a]	67.83 ± 0.23[a]	1.92[a]	$Y = 0.0554\ ST^2 - 0.5904\ ST + 66.997$	0.974
pH					
CCFs	5.83 ± 0.00[c]	6.19 ± 0.06[b]	6.17[a]	$Y = 0.0058\ ST^2 - 0.0418\ ST + 5.8596$	0.995
UCCFs	6.03 ± 0.01[b]	6.40 ± 0.04[a]	6.13[a]	$Y = 0.0046\ ST^2 - 0.0250\ ST + 6.0424$	0.999
Acidity (% acid)					
CCFs	1.64 ± 0.23[a]	0.85 ± 0.01[b]	48.17[a]	$Y = -0.0152\ ST^2 + 0.1359\ ST + 1.455$	0.901
UCCFs	1.52 ± 0.25[a]	0.69 ± 0.05[b]	54.60[a]	$Y = -0.0241\ ST^2 + 0.2361\ ST + 1.321$	0.997
TBARS (mg MDA/kg)					
CCFs	0.263 ± 0.01[c]	2.01 ± 0.38[b]	664.2[b]	$Y = 0.0652\ ST^2 - 0.4549\ ST + 1.036$	0.938
UCCFs	0.367 ± 0.01[c]	5.15 ± 0.84[a]	1,303[a]	$Y = 0.1561ST + 0.024$	0.972
Colour L^*-value					
CCFs	78.16 ± 0.51[a]	70.06 ± 1.34[b]	10.36[a]	$Y = 0.0834\ ST^2 - 1.836\ ST + 80.011$	0.997
UCCFs	70.85 ± 0.79[b]	63.21 ± 2.62[c]	10.78[a]	$Y = -2.966\ \ln(ST) + 70.68$	0.981
Colour a^*-value					
CCFs	0.27 ± 0.04[d]	4.91 ± 0.72[b]	1,918[a]	$Y = 0.2861\ ST^{1.3133}$	0.926
UCCFs	1.60 ± 0.65[c]	14.09 ± 2.42[a]	780.6b	$Y = -0.2256\ ST^2 + 3.8996\ ST - 0.9571$	0.871
Colour b^*-value					
CCFs	1.01 ± 0.08[d]	22.02 ± 0.42[b]	2,080[a]	$Y = 0.8218\ ST^{1.3526}$	0.903
UCCFs	5.38 ± 0.26[c]	32.06 ± 4.79[a]	495.9[b]	$Y = -0.4177\ ST^2 + 7.5823\ ST + 0.026$	0.919
ΔE					
CCFs	8.77 ± 0.13[c]	17.00 ± 0.67[b]	93.84[b]	$Y = 1.0698\ ST + 5.5564$	0.600
UCCFs	0.00 ± 0.00[d]	27.50 ± 2.79[a]	2,750[a]	$Y = -0.4612\ ST^2 + 8.1038\ ST - 5.0426$	0.850
Hardness (N)					
CCFs	14.49 ± 1.11[a]	8.77 ± 0.98[c]	39.47[b]	$Y = -0.7417\ ST + 15.555$	0.990
UCCFs	11.76 ± 0.57[b]	4.60 ± 1.03[c]	60.88[a]	$Y = -0.3304\ ST + 12.388$	0.940
Sensory odor/flavor					
CCFs	8.33 ± 0.57[a]	5.50 ± 0.09[b]	33.97[a]	$Y = -0.2313\ ST + 8.3609$	0.915
UCCFs	7.33 ± 0.57[a]	5.16 ± 0.28[b]	29.60[a]	$Y = -0.1968\ ST + 7.3927$	0.974
Sensory texture					
CCFs	7.66 ± 0.57[a]	6.00 ± 0.00[a]	21.67[b]	$Y = -0.1468\ ST + 7.7073$	0.981
UCCFs	7.26 ± 0.52[a]	5.16 ± 0.27[b]	28.92[a]	$Y = -0.1717\ ST + 7.2182$	0.907
Sensory colour					
CCFs	8.33 ± 0.47[a]	6.02 ± 0.06[b]	27.73[a]	$Y = -0.2089\ ST + 8.4355$	0.987
UCCFs	7.66 ± 0.23[a]	5.66 ± 0.05[b]	28.92[a]	$Y = -0.1796\ ST + 7.6873$	0.965
Overall acceptability					
CCFs	8.41 ± 0.21[a]	6.98 ± 0.16[b]	17.00[b]	$Y = -0.132\ ST + 8.43$	0.946
UCCFs	7.21 ± 0.61[a]	5.02 ± 0.28[c]	30.37[a]	$Y = -0.205\ ST + 7.3464$	0.976

[a] UCCFs and CCFs are the uncoated and coated chicken fillets, respectively.
[b] Values in rows related to each the quality property in storage days followed by different letters are significantly different ($p < 0.05$).
[c] Values in the same column for each the quality property followed by different letters are significantly different ($p < 0.05$).
[d] ST, Storage time; The trend line was fitted by the Excel 2007 software.

TBARS and all the organoleptic traits. No significant difference in the moisture content of CCFs and UCCFs at the initial and final storage days was observed (Table 3). An increase in pH, redness and yellowness values and a reduction in amounts of acidity and lightness, were determined by prolonging the storage period ($p < 0.05$). Although the trained panelists reported that the all samples stored for 12 days had worse sensory scores than the initial storage day ($p < 0.05$), no significant change in the sensory scores of texture for CCFs with increasing the storage time was detected (Table 3). On the other hand, a linear equation (R^2, 0.907–0.987) was well fitted with the experimental data of sensory characteristics of CCFs and UCCFs, while other quality parameters were mostly fitted with polynomial equations with high R^2 (Table 3).

In general, edible coatings developed based on polysaccharides as strong barriers by reducing the moisture diffusion coefficient maintain the surface water activity of meat products during the storage period (Kester and Fennema, 1986). Therefore, insignificantly more moisture levels in CCFs compared to UCCFs can be due to the physical barrier character of S-NCs. More acidity or lower pH of CCFs compared to UCCFs is mainly owing to the phenolic compounds present in SLPE and the nature of S-NCs. The phenolic acids can easily produce acidic aquoues solutions in the presence of S-NCs crystalline structures. Phenolics by quenching free radicals causing the lipid and protein oxidation process led to a lower TBARS value in CCFs than UCCFs. Furthermore, S-NCs by protecting phenolics and even flavonoids against various degradative reactions can significantly improve the antioxidant potential during the storage (Naveena et al., 2010). Therefore, coating solutions through retarding the oxidation processes of lipids and proteins and probably reducing the microbial degradation rate can notably ensure the maintenance of favorable colour attributes for chicken fillets. Besides, decreasing the accessibility rate of endogenous enzymes and microorganisms to myofibrillar and collagen proteins in CCFs can effectively prevent the structural breakdown and textural softening (Gharibzahedi and Mohammadnabi, 2017). Higher scores of sensory characteristics in CCFs at the initial storage time and also their lower changes during the cold-storage than UCCFs may be attributed to the more surface moisture and lightness amounts, lower development of

products caused by the oxidation of lipids and proteins (e.g., ammonia) and thus less off-odor and off-flavor (Bazargani-Gilani et al., 2015).

4. Conclusion

The effectiveness of S-NC based coating solutions incorporated with aqueous SLPE to improve the physico-chemical, textural and sensorial quality of chicken fillets during 14-d cold storage was investigated. The optimization studies showed that the transparent coating solutions containing 4.0% S-NC and 5.62% SLPE mixed at 51.17 °C for 43.29 min can well provide the high antimicrobial and antioxidant capacity to prevent the microbial spoilage and oxidative deterioration during the storage. As a result, the active combined substances in the present work may be applied to prolong the shelf life of other protein-based food materials. In addition, further evaluations should be directed towards the formation of coating solutions with different sour lemon varieties and starch origins and their effects on the functionality of final edible coatings.

References

Angellier, H., Choisnard, L., Molina-Boisseau, S., Ozil, P., Dufresne, A., 2004. Optimization of the preparation of aqueous suspensions of waxy maize starch nanocrystals using a response surface methodology. Biomacromolecules 5, 1545–1551.

AOAC, 2005. Association of Official Analytical Chemists, Official Methods of Analysis, 18th edn. (Gaithersburg, Maryland).

Basiak, E., Lenart, A., Debeaufort, F., 2017. Effect of starch type on the physico-chemical properties of edible films. Int. J. Biol. Macromol. 98, 348–356.

Bazargani-Gilani, B., Aliakbarlu, J., Tajik, H., 2015. Effect of pomegranate juice dipping and chitosan coating enriched with *Zataria multiflora* Boiss essential oil on the shelf-life of chicken meat during refrigerated storage. Innov. Food Sci. Emerg. Technol. 29, 280–287.

Bocco, A., Cuvelier, M.E., Richard, H., Berset, C., 1998. Antioxidant activity and phenolic composition of citrus peel and seed extracts. J. Agric. Food Chem. 46, 2123–2129.

Bof, M.J., Jiménez, A., Locaso, D.E., García, M.A., Chiralt, A., 2016. Grapefruit seed extract and lemon essential oil as active agents in corn starch–chitosan blend films. Food Bioprocess Technol. 9, 2033–2045.

Burt, S., 2004. Essential oils: their antibacterial properties and potential applications in food-a review. Int. J. Food Microbiol. 94, 223–253.

Choulitoudi, E., Bravou, K., Bimpilas, A., Tsironi, T., Tsimogiannis, D., Taoukis, P., Oreopoulou, V., 2016. Antimicrobial and antioxidant activity of *Satureja thymbra* in gilthead seabream fillets edible coating. Food Bioprod. Process. 100, 570–577.

Condés, M.C., Añón, M.C., Mauri, A.N., Dufresne, A., 2015. Amaranth protein films reinforced with maize starch nanocrystals. Food Hydrocoll. 47, 146–157.

Garavand, F., Madadlou, A., 2014. Recovery of phenolic compounds from effluents by a microemulsion liquid membrane (MLM) extractor. Colloids Surf. A Physicochem. Eng. Asp. 443, 303–310.

Garavand, F., Rouhi, M., Razavi, S.H., Cacciotti, I., Mohammadi, R., 2017. Improving the integrity of natural biopolymer films used in food packaging by crosslinking approach: a review. Int. J. Biol. Macromol. 104, 687–707.

Ge, Y., Duan, G., Fang, Zhang, Y., and Wang, S., 2009. Polysaccharides from fruit calyx of Physalis alkekengi var. francheti: isolation, purification, structural features and antioxidant activities. Carbohydr. Polym. 77, 188–193.

Ge, S., Xiong, L., Li, M., Liu, J., Yang, J., Chang, R., Liang, C., Sun, Q., 2017. Characterizations of Pickering emulsions stabilized by starch nanoparticles: influence of starch variety and particle size. Food Chem. 234, 339–347.

Gharibzahedi, S.M.T., 2017. Ultrasound-mediated nettle oil nanoemulsions stabilized by purified jujube polysaccharide: process optimization, microbial evaluation and physicochemical storage stability. J. Mol. Liq. 234, 240–248.

Gharibzahedi, S.M.T., Mohammadnabi, S., 2016. Characterizing the novel surfactant-stabilized nanoemulsions of stinging nettle essential oil: thermal behaviour, storage stability, antimicrobial activity and bioaccessibility. J. Mol. Liq. 224, 1332–1340.

Gharibzahedi, S.M.T., Mohammadnabi, S., 2017. Effect of novel bioactive edible coatings based on jujube gum and nettle oil-loaded nanoemulsions on the shelf-life of Beluga sturgeon fillets. Int. J. Biol. Macromol. 95, 769–777.

Gharibzahedi, S.M.T., Mousavi, S.M., Hamedi, M., Khodaiyan, F., Razavi, S.H., 2012. Development of an optimal formulation for oxidative stability of walnut-beverage emulsions based on gum arabic and xanthan gum using response surface methodology. Carbohydr. Polym. 87, 1611–1619.

Gharibzahedi, S.M.T., Razavi, S.H., Mousavi, S.M., 2015a. Optimization and kinetic studies on the production of intracellular canthaxanthin in fed-batch cultures of *Dietzia natronolimnaea* HS-1. Qual. Assur. Saf. Crops Food 7, 757–767.

Gharibzahedi, S.M.T., Rostami, H., Yousefi, S., 2015b. Formulation design and physicochemical stability characterization of nanoemulsions of nettle (*Urtica dioica*) essential oil using a model-based methodology. J. Food Process. Preserv. 39, 2947–2958.

González, K., Retegi, A., González, A., Eceiza, A., Gabilondo, N., 2015. Starch and cellulose nanocrystals together into thermoplastic starch bionanocomposites. Carbohydr. Polym. 117, 83–90.

Hari, N., Shaji, K., Radhakrishnan, S., Nair, A.J., 2017. Physico-chemical and biological properties of starch nanocrystals and orange oil incorporated chitosan film. J. Polym. Mater. 34, 261–274.

Jiang, S., Liu, C., Han, Z., Xiong, L., Sun, Q., 2016. Evaluation of rheological behavior of starch nanocrystals by acid hydrolysis and starch nanoparticles by self-assembly: a comparative study. Food Hydrocoll. 52, 914–922.

Jivan, M.J., Madadlou, A., Yarmand, M., 2013. An attempt to cast light into starch nanocrystals preparation and cross-linking. Food Chem. 141, 1661–1666.

Kargar, M., Fayazmanesh, K., Alavi, M., Spyropoulos, F., Norton, I.T., 2012. Investigation into the potential ability of Pickering emulsions (food-grade particles) to enhance the oxidative stability of oil-in-water emulsions. J. Colloid Interface Sci. 366, 209–215.

Kester, J.J., Fennema, O., 1986. Edible films and coatings: a review. Food Technol. 40, 47–59.

Khare, A.K., Abraham, R.J., Rao, V.A., Babu, R.N., Ruban, W., 2017. Effect of chitosan and cinnamon oil edible coating on shelf life of chicken fillets under refrigeration conditions. Indian J. Anim. Res. 51, 603–610.

Kurup, T.R., Wan, L.S., Chan, L.W., 1991. Effect of surfactants on the antibacterial activity of preservatives. Pharm. Acta Helv. 66, 274–280.

Latou, E., Mexis, S.F., Badeka, A.V., Kontakos, S., Kontominas, M.G., 2014. Combined effect of chitosan and modified atmosphere packaging for shelf life extension of chicken breast fillets. LWT Food Sci. Technol. 55, 263–268.

Le Corre, D., 2011. Starch Nanocrystals: Preparation and Application to Bio-based Flexible Packaging. Doctoral dissertation. Université de Grenoble.

Lethuaut, L., Métro, F., Genot, C., 2002. Effect of droplet size on lipid oxidation rates of oil-in-water emulsions stabilized by protein. J. Am. Oil Chem. Soc. 79, 425–430.

Li, C., Sun, P., Yang, C., 2012. Emulsion stabilized by starch nanocrystals. Starke 64, 497–502.

Li, C., Li, Y., Sun, P., Yang, C., 2014. Starch nanocrystals as particle stabilisers of oil-in-water emulsions. J. Sci. Food Agric. 94, 1802–1807.

Liang, R., Jiang, Y., Yokoyama, W., Yang, C., Cao, G., Zhong, F., 2016. Preparation of Pickering emulsions with short, medium and long chain triacylglycerols stabilized by starch nanocrystals and their in vitro digestion properties. RSC Adv. 6, 99496–99508.

Lin, N., Huang, J., Chang, P.R., Anderson, D.P., Yu, J., 2011a. Preparation, modification, and application of starch nanocrystals in nanomaterials: a review. NanoImpact 2011, 573687.

Lin, N., Huang, J., Chang, P.R., Feng, L., Yu, J., 2011b. Effect of polysaccharide nanocrystals on structure, properties, and drug release kinetics of alginate-based microspheres. Colloids Surf. B 85, 270–279.

Lozano-Navarro, J. I., Díaz-Zavala, N. P., Velasco-Santos, C., Martínez-Hernández, A. L., Tijerina-Ramos, B. I., García-Hernández, M., et al., 2017. Antimicrobial, optical and mechanical properties of chitosan–starch films with natural extracts. Int. J. Mol. Sci. 18, 997.

Moghaddam, A.D., Garavand, F., Razavi, S.H., Talatappe, H.D., 2018. Production of saffron-based probiotic beverage by lactic acid bacteria. J. Food Meas. Charact. 12, 2708–2717.

Mukurumbira, A.R., Mellem, J.J., Amonsou, E.O., 2017. Effects of amadumbe starch nanocrystals on the physicochemical properties of starch biocomposite films. Carbohydr. Polym. 165, 142–148.

Natseba, A., Lwalinda, I., Kakura, E., Muyanja, C.K., Muyonga, J.H., 2005. Effect of pre-freezing icing duration on quality changes in frozen Nile perch (*Latesniloticus*). Food Res. Int. 38, 469–474.

Naveena, B., Sen, A., Vaithiyanathan, S., Patil, G., Kondaiah, N., 2010. Antioxidant potential of pomegranate juice in cooked chicken patties. J. Muscle Foods 21, 557–569.

Nychas, G.J.E., Skandamis, P.N., Tassou, C.C., Roller, S., 2003. Antimicrobials from herbs and spices. In: Roller, S. (Ed.), Natural Antimicrobials for the Minimal Processing of Foods. CRC Press, Boca Raton, USA, pp. 176–200.

Owens, C.M., Alvarado, C.Z., Sams, A.R., 2010. Poultry Meat Processing, 2nd edition. CRC Press, Boca Raton.

Rostami, H., Gharibzahedi, S.M.T., 2017. Cellulase-assisted extraction of polysaccharides from *Malva sylvestris*: process optimization and potential functionalities. Int. J. Biol. Macromol. 101, 196–206.

Ruiz, V.E., Interdonato, R., Cerioni, L., Albornoz, P., Ramallo, J., Prado, F.E., Hilal, M., Rapisarda, V.A., 2016. Short-term UV-B exposure induces metabolic and anatomical changes in peel of harvested lemons contributing in fruit protection against green mold. J. Photochem. Photobiol. B Biol. 159, 59–65.

Umaraw, P., Verma, A.K., 2017. Comprehensive review on application of edible film on meat and meat products: an eco-friendly approach. Crit. Rev. Food Sci. Nutr. 57, 1270–1279.

Vatankhah, M., Garavand, F., Mohammadi, B., Elhamirad, A., 2017. Quality attributes of reduced-sugar Iranian traditional sweet bread containing stevioside. J. Food Meas. Charact. 11, 1233–1239.

Viguie, J., Molina-Boisseau, S., Dufresne, A., 2007. Processing and characterization of waxy maize starch films plasticized by sorbitol and reinforced with starch nanocrystals. Macromol. Biosci. 7, 1206–1216.

Xu, G.H., Chen, J.C., Liu, D.H., Zhang, Y.H., Jiang, P., Ye, X.Q., 2008. Minerals, phenolic compounds, and antioxidant capacity of citrus peel extract by hot water. J. Food Sci. 73, C11–C18.

Yousefi, S., Emam-Djomeh, Z., Mousavi, M., Kobarfard, F., Zbicinski, I., 2015. Developing spray-dried powders containing anthocyanins of black raspberry juice encapsulated based on fenugreek gum. Adv. Powder Technol. 26, 462–469.

Zhang, X., Huang, J., Chang, P.R., Li, J., Chen, Y., Wang, D., Yu, J., Chen, J., 2010. Structure and properties of polysaccharide nanocrystal-doped supramolecular hydrogels based on cyclodextrin inclusion. Polymer 51, 4398–4407.